Analysis of the Effect of Control Bandwidth on Inverter Interactions Using Small-Signal Stability Analysis

Luis I. de la Barba
Instituto de Investigación Tecnológica (IIT)
ETSI ICAI, Universidad Pontificia Comillas
Madrid, Spain
luis.delabarba @iit.comillas.edu

Lukas Sigrist
Instituto de Investigación Tecnológica (IIT)
ETSI ICAI, Universidad Pontificia Comillas
Madrid, Spain
lukas.sigrist @iit.comillas.edu

Luis Rouco
Instituto de Investigación Tecnológica (IIT)
ETSI ICAI, Universidad Pontificia Comillas
Madrid, Spain
luis.rouco @iit.comillas.edu

Régulo Ávila-Martínez
Instituto de Investigación Tecnológica (IIT)
ETSI ICAI, Universidad Pontificia Comillas
Madrid, Spain
regulo.avila @iit.comillas.edu

Aurelio Garcia-Cerrada
Instituto de Investigación Tecnológica (IIT)
ETSI ICAI, Universidad Pontificia Comillas
Madrid, Spain
aurelio.garcia @iit.comillas.edu

***Abstract*— The penetration of power inverter connected renewable energy sources in the grid and in particular in distribution grids is growing day by day. This paper investigates, the stability of converters interacting in electrical islands through a small-signal model. More precisely, the impact of the bandwidth of the cascaded inverter controls of inverters operating in islanded grids is addressed by using modal analysis. The study relies on a detailed fundamental model of the power inverter and grid dynamics. The study shows that control interactions depend to a large extent on the system configuration, i.e., whether grid-forming and/or grid-feeding inverters are present in the islanded grid.**

***Keywords*— Grid-forming inverter, grid-feeding inverter, pole placement, modal analysis, eigenvalues.**

I. INTRODUCTION

The penetration of power inverter connected renewable energy sources in the grid and in particular in distribution grids is growing day by day. Meanwhile, a growing number of unintentional islanding events of parts of distribution grids involving inverter-connected generation has being reported [1]. Although islanded operation could be maintained if sufficient controllable resources exist in the island, the transition from interconnected to islanded operation and islanded operation itself pose several technical challenges and is currently not allowed. These challenges have their roots in the fact that islanded parts of the grid are small, weak low inertia systems with a limited number of controllable resources. In this scenario, among other problems, undesired interactions of the controls of inverter-based generation are likely to occur.

Inverter-connected generation can be broadly classified into grid-feeding (GFeed) or grid-following and grid-forming (GForm) inverters according to their operation mode. The control of grid-following inverters ensures the injection of given active and reactive powers values by synchronizing the inverter and its controls with the grid, requiring the presence of a sufficiently strong grid and a phase-locked loop (PLL). By contrast, grid-forming inverters can adjust the imposed voltage and frequency according to the active and reactive power measured, for instance through droop controls, virtual synchronous machine implementation, etc. ([2]). Grid-forming inverters are commonly used for batteries, whereas grid-feeding inverters are used for PV generation.

Inverter control typically shows a cascade structure involving current-control loops, voltage-control loops, and power-control loops according to the inverter's operation mode [3]. Controls are typically implemented in stationary or synchronous reference frames by using Proportional+Resonant (PR) or Proportional+Integral (PI) controllers, respectively.

A major difficulty dwells in the design of the PR and PI controllers in order to obtain a stable response under different operating conditions. Many solutions have been proposed, but currently there is no universal methodology for designing robust controls under different scenarios [4]. Furthermore, the interconnection of different inverters through rather weak grids might provoke interactions which may cause the system to become unstable although the individual design of the parameters of each converter predicted a stable system.

Reference [5] discusses different methods, including "Modulus optimum", "Symmetrical optimal" or "Pole placement" to tune controller parameters to obtain robust and fast responses in inverters. However, these methods do not take into account the interaction of the inverter and its control with the rest of the system. Alternatively, other papers suggest design methods taking into account the whole system ([3], [4], [6]). For example, in reference [6] the author presents a methodology based on parameter iteration. In this iteration the author changes the control parameters automatically in the simulations until the resulted eigenvalues are far enough from the instability region. Meanwhile, [8] uses eigenvalue and participation analysis to detect which parameter must be changed to guarantee overall stability of the system. These criteria have the drawback that they need a detailed knowledge of the whole system prior the design.

Hence, although there are many design methodologies and studies, control interactions of multiple, different inverters are a challenge for distribution grids that might operate in islanded

mode. Along these lines, this paper investigates the small signal stability of multiple inverters by using a fundamental and detailed model which includes full electromagnetic representation of the grid and the controllers applied to the inverters. Eigenvalues and participation factors are obtained and discussed in detail to analyze the stability. Small-signal analysis has already been used to assess microgrid stability with grid-forming inverters in [7] and [8]. The former proposes a small signal process to modeling systems and studies the impact of the droop controllers in the overall stability whereas the latter studies the impact of the transmission grid. The current paper intends to contribute to the study of the interaction between grid-feeding and grid-forming inverters with special focus on the controller bandwidth.

To this end, the paper:

- implements a method based on pole placement to tune controller parameters.
- analyses the control interactions of different system configurations, i.e., different combinations of grid-forming and grid-feeding inverters connected in parallel.
- carries out a sensitivity analysis of the results with respect to control bandwidth.

The rest of the paper is organized as follows, Section II explains the model, the design methodology and the small signal analysis procedure. Section III makes a brief introduction to the test performed, and Section IV presents the results when analyzing the control interactions between grid-feeding and grid-forming inverters, and among grid-forming inverters. Finally, Section V summarizes the main conclusions of the paper.

II. INVERTER MODELING AND PARAMETER TUNNING

This paper studies the control interactions between inverters. For the modeling, a power inverter, suitable to work as GFeed or GForm, with an LCL filter is depicted in Fig. *1*. Here, models and controllers will be referred to synchronously rotating frame with its d axis aligned with the voltage of the LCL filter capacitor. First of all, modeling of components and controls common to both, GFeed and GForm inverters are presented. Secondly, specific controls of GForm and GFeed inverters are introduced. Finally, the tuning methodology employed is explained.

A. Common system modeling

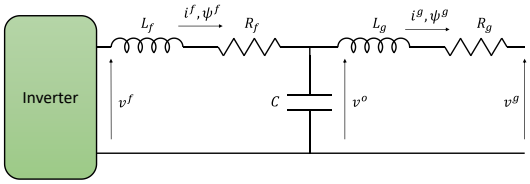

Fig. 1 Hardware structure employed in the models.

Input inductance (L_f, R_f) and the capacitor (C) of the LCL filter are typically filter elements, meanwhile the output inductance (L_g, R_g) typically represents an inductor in combination with a line inductance or a transformer. This filter in Fig. *1*is described, in a d-q reference frame, as follows

$$\begin{aligned} \dot{\psi}_d^f &= \omega_0 \cdot (v_d^f - v_d^o - R_f \cdot i_d^f + \boldsymbol{j} \cdot \omega_{ref} \cdot \psi_d^f) \\ \dot{\psi}_q^f &= \omega_0 \cdot (v_q^f - v_q^o - R_f \cdot i_q^f - \boldsymbol{j} \cdot \omega_{ref} \cdot \psi_q^f) \end{aligned} \quad (1)$$

$$\begin{aligned} \psi_d^f &= L_f \cdot i_d^f \\ \psi_q^f &= L_f \cdot i_q^f \\ \dot{v_d^o} &= \omega_0 \cdot (\frac{1}{C} \cdot i_d^f + \boldsymbol{j} \cdot \omega_{ref} \cdot v_d^o) \\ \dot{v_q^o} &= \omega_0 \cdot (\frac{1}{C} \cdot i_q^f - \boldsymbol{j} \cdot \omega_{ref} \cdot v_q^o) \end{aligned} \quad (2)$$

$$\begin{aligned} \dot{\psi_d^g} &= \omega_0 \cdot (v_d^o - v_d^g - R_g \cdot i_d^g + \boldsymbol{j} \cdot \omega_{ref} \cdot \psi_q^g) \\ \dot{\psi_q^g} &= \omega_0 \cdot (v_q^o - v_q^g - R_g \cdot i_q^g - \boldsymbol{j} \cdot \omega_{ref} \cdot \psi_d^g) \end{aligned} \quad (3)$$

where v^f, v^0, and v^g are the fundamental voltages of the inverter, the capacitor and of the grid, respectively. i^f, i^g, ψ^f, and ψ^g denote the inverter and the grid current and their associated flux linkage values in inductors L_f and L_g. ω_0 is the base angular speed in rad/s and ω_{ref} is the angular speed of the $d-q$ reference frame in pu.

A current control (CC) is often used as the inner control loop to limit the inverter current and to improve the controllability of the system. Since the model is formulated in a synchronous reference frame, PI controllers are used to control the d-axis and q-axis current components. The equivalent transfer function of the PWM of the inverter can be omitted if the current control is sufficiently slow with respect to the switching frequency of the PWM.

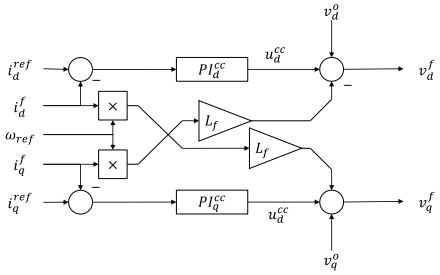

Fig. 2 Current Control block diagram.

Fig. *2*, shows a block diagram of the typical current control employed. The block diagram shows the PI controllers, and the terms to decouple d- and q-axis dynamics. Lastly, the capacitor voltage (v^o) is also considered.

B. GForm-specific model

GForm inverters can adjust the imposed frequency and voltage in response to changes in the active and reactive powers consumed by the rest of the system. A power-control loop gives the set point for the frequency of the inverter and for the d-axis component of the capacitor voltage for the underlying voltage control (VC) loop. The power control is often based on a droop control. The voltage control gives the set-point values for the d-axis and q-axis currents to be used in the current control loop.

1) Voltage Control (VC)

The VC used follows the same structure as the CC (see Fig. *3*). PI controllers are used and feedforward terms of the capacitor voltage (v^o) are applied. Those terms will be added to the PI response to obtain the final output which will be be applied to the CC (i^{ref}).

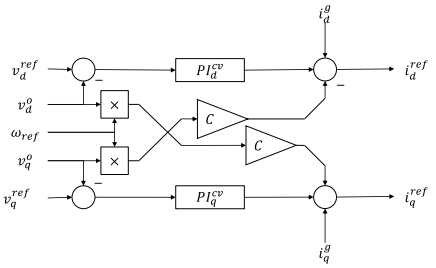

Fig. 3 Voltage Control block diagram of the GForm inverter.

2) Droop control

Fig. *4* shows the droop control used. Active and reactive power measurements are passed through a low-pass filter before the droop is applied. Then, set-point values ω_{ref} and v_d^{ref} are computed from the output set points of active power (P^*), reactive power (Q^*) and voltage (v_d^{ref}).

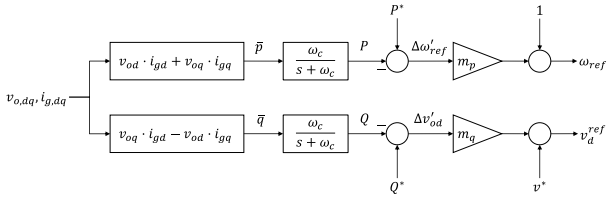

Fig. 4 Droop Control diagram of the GForm inverter.

C. GFeed-specific model

GFeed inverters are generally used for inverter-connected renewable energy sources. Their main purpose is to pass all the available power from to source to the grid. They synchronize with the grid through a PLL. GFeed inverters cannot operate in stand-alone mode since they cannot impose either frequency or voltage. They require the presence of the grid or at least of a GForm inverter.

1) Phase Looked Loop (PLL)

A PLL synchronizes the control with the grid and assures that, at least in steady state, the d-axis of the synchronous reference frame is aligned with the capacitor voltage. Fig. *5* shows a simple implementation of a PLL.

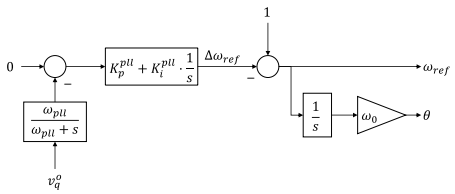

Fig. 5 PLL block diagram.

2) Power Injection

Set points for d-axis and q-axis currents of the CC are set here through an open-loop calculation from the active- and reactive-power set points (P^*) and (Q^*), respectively (see Fig. *6*). A closed-loop active and reactive power control or even a DC-link voltage control loop could be used instead.

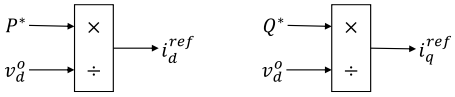

Fig. 6 Grid Feeder Power injection diagram

D. Controller design methodology

Inner current controllers are identical in GForm and GFeed inverters. Assuming that d-q dynamics decoupling works accurately, the closed loop transfer functions of the d- and q-axis control systems will take the form:

$$F^{cc}(s) = \frac{I_{d/q}(s)}{I_{d/q}^{ref}(s)} = \frac{\frac{K_p^{cc}\cdot\omega_0}{L_f}\cdot s + \frac{K_i^{cc}\cdot\omega_0}{L_f}}{s^2 + \frac{R_f\cdot\omega_0 + K_p^{cc}\cdot\omega_0}{L_f}\cdot s + \frac{K_i^{cc}\cdot\omega_0}{L_f}} \quad (4)$$

and have been designed to have natural frequency frequencies (ω_n^{cc})and damping coefficients as shown in Table 1.

TABLE 1 CURRENT CONTROL DESIGN PARAMETERS

Parameter		Value
GFeed	$\boldsymbol{\omega_n^{cc}}$	1250
	$\boldsymbol{\zeta}$	0.7
GForm	$\boldsymbol{\omega_n^{cc}}$	1000
	$\boldsymbol{\zeta}$	0.7

Lastly, the outer controller of the GForm, the VC have been designed assuming that the inner current controller is much faster than the outer ones, in order of one decade, and can be approximated by a first-order transfer function as:

$$F_{cc}(s) = \frac{1}{T_1 s + 1} \quad (5)$$

The closed-loop voltage of the GForm controller will then take the form of:

$$F^{cv}(s) = \frac{\frac{K_p^{cv}\cdot\omega_0}{C_f\cdot T_1}\cdot s + \frac{K_i^{cv}\cdot\omega_0}{C_f\cdot T_1}}{s^3 + \frac{1}{T_1}\cdot s^2 + \frac{K_p^{cv}\cdot\omega_0}{C_f\cdot T_1}\cdot s + \frac{K_i^{cv}\cdot\omega_0}{C_f\cdot T_1}} \quad (6)$$

The characteristic polynomial of transfer functions (7) and (6) $(p_{VC}(s))$and $(p_{CC}(s))$can be written as:

$$p_{xx}(s) = (T_s s + 1)(s^2 + 2\omega_n\zeta s + \omega_n^2) \quad (7)$$

and the controller parameters have been designed to achieve the closed loop parameters shown in Table 2, except T_s, which will be calculated in function of the other variables as

$$T_s = \frac{T_1}{1 - 2\cdot\zeta\cdot\omega_n\cdot T_1} \quad (8)$$

Table 2 shows the design objectives for the GForm CV. It is remarkable that $\omega_n^{cc} = 10\cdot\omega_n^{cv}$ to achieve a faster response of the CC.

TABLE 2 VOLTAGE CONTROL DESIGN PARAMETERS

Parameter		Value
GForm	$\boldsymbol{\omega_n^{cc}}$	100
	$\boldsymbol{\zeta}$	1.0

E. Parameters

Parameters of the GForm and the GFeed are collected in Table 3 and Table 4, including the controllers calculated using the methodology in Section II.D.

TABLE 3 GRID FORMER PARAMETERS

Parameter	Value	Parameter	Value (pu)
$\boldsymbol{L_f}$	0.2000 pu	$\boldsymbol{m_p}$	0.0110 pu
$\boldsymbol{R_f}$	0.0200 pu	$\boldsymbol{m_q}$	0.0800 pu
$\boldsymbol{C}$	0.1000 pu	$\boldsymbol{P^*}$	0.5000 pu

L_g	0.0600 pu	Q^*	0.3240 pu
R_g	0 pu	ω^{ref}	1.0000 pu
K_p^{cc}	0,8713 pu	v^{ref}	1.0184 pu
K_i^{cc}	636,6198 pu	ω_c	20 rad/s
K_p^{cv}	0,0503 pu	ω_0	314,1593 rad/s
K_i^{cv}	2,2918 pu		

TABLE 4 GRID FEEDER PARAMETERS

Parameter	Value	Parameter	Value
L_f	0.2000 pu	K_p^{pll}	0.3979 pu
R_f	0.0200 pu	K_i^{pll}	4.7746 pu
C	0.1000 pu	ω_{pll}	500 rad/s
L_g	0.0600 pu	P^*	0.5000 pu
R_g	0 pu	Q^*	0.0851 pu
K_p^{cc}	1.0941 pu	ω_0	314.1593 rad/s
K_i^{cc}	2.2918 pu		

F. *Small-signal and Modal Analysis*

Modal analysis is proposed to assess the small-signal stability of the models. Modal analysis calculates not only the eigenvalues but also the right and left eigenvectors of the state matrix $\boldsymbol{A}$. From the right and left eigenvectors, participation factors can be easily calculated to find the relationships between eigenvalues and state variables.

The right and left eigenvectors ($\boldsymbol{v}_i$ and $\boldsymbol{w}_i$ respectively) corresponding to the eigenvalue $\boldsymbol{\lambda}_i$ of the state matrix $\boldsymbol{A}$ are defined according to

$$\begin{aligned} \boldsymbol{A}\boldsymbol{v}_i &= \boldsymbol{v}_i\boldsymbol{\lambda}_i \\ \boldsymbol{w}_i^T\boldsymbol{A} &= \boldsymbol{\lambda}_i\boldsymbol{w}_i^T \end{aligned} \tag{9}$$

The participation factor [9] of the j-th variable in the i-th mode is defined as

$$\boldsymbol{p}_{ji} = \boldsymbol{w}_{ji}\boldsymbol{v}_{ji} \tag{10}$$

III. CASES TO BE STUDIED

The study carried out has focus on the interaction of

a) a GForm inverter with a GFeed inverter

b) a GForm inverter and a GForm inverter

in an island configuration without any connection to an external grid. The sensitivity analysis has been carried out changing ω_n^{cc} and therefore ω_n^{cv} to maintain the $\omega_n^{cc} = 10 \cdot \omega_n^{cv}$ diference.

The models will be connected in through a bus with a load formed by an impedance (Z) made by a resistance (R_s) and a inductance (L_s) in series with a capacitor (C) in parallel. Additionally, in order to make the model work, the system is referenced to one of the GForms whereas the other modules are rotated in function to the reference.

IV. RESULTS

A. *Grid Former – Grid Feeder*

Fig. 7 shows the single line diagram of the GFrom inverter – GFeed inverter configuration. The inverters are connected in parallel to a single bus with a series inductance and resistance in parallel with a capacitor load with the parameters in Table 5. Parameters of the GForm and GFeed inverters are shown in Table 3 and Table 4. Initial active and reactive power injections of the GForm inverter are 0.5 and 0.324 pu respectively, whereas the GFeed inverter injects 0.5 pu active power and 0.0851 pu reactive power. The load is such that it consumes the active power provided by the inverters and the reactive power is compensated to obtain a bus voltage of 1 pu.

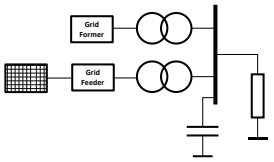

Fig. 7 Single line diagram for GFeed-GForm configuration.

TABLE 5 VALUES OF THE LOAD

Parameter		Value
Z	R_s	0.9123 pu
	L_s	0.2828 pu
C		0.0100 pu

Table 6 and Table 7 show the complex and real eigenvalues of the system shown in Fig. *7*. Since all the real parts of the eigenvalues have negative values, the initial system is stable. However, modes 1 and 3 exhibit low damping ratio.

TABLE 6 COMPLEX EIGENVALUES

Complex				
No.	Real	Imag.	Damp. (%)	Freq. (Hz)
1	-58,20	19775,68	0,29	3147,40
3	-58,44	19147,40	0,31	3047,40
5	-325,62	4457,16	7,29	709,38
7	-366,52	3832,94	9,52	610,03
9	-723,27	1982,83	34,27	315,58
11	-732,32	1313,57	48,69	209,06
13	-875,00	892,68	70,00	142,07
15	-788,59	592,94	79,93	94,37
18	-88,80	154,01	49,95	24,51
20	-76,44	101,44	60,18	16,15
22	-74,10	25,75	94,46	4,10
25	-20,40	1,65	99,68	0,26

TABLE 7 REAL EIGENVALUES

Real	
No.	Real
17	-406,85
24	-71,44
27	-13,17

Table 8 shows the participation factors of each mode as described in (10), indicating the relative activity of a mode in each state variable. The two weakly damped modes relate to the network, i.e., the state variables related to the output inductance (L_g) and the RLC load. The control-related state variables for the GForm inverter are $\{\boldsymbol{x}_d^o, \boldsymbol{x}_q^o, \boldsymbol{x}_d^i, \boldsymbol{x}_q^i\}$ and for the GFeed inverter $\{\boldsymbol{x}_d^i, \boldsymbol{x}_q^i\}$. Those variables relate to several modes. Modes 22 and 24 have an important activity in the VC-related state variables of the GForm inverter.

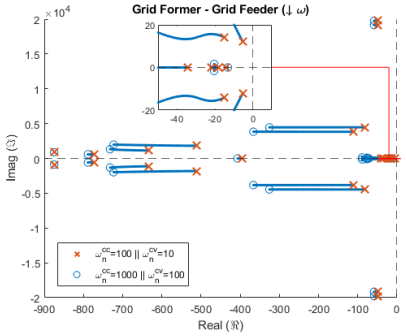

Fig. 8 Eigenvalue locus trajectories in function of the reduction of the control bandwidth modifying the GForm of a GForm-GFeed system.

Finally, the impact of varying the bandwidth of the CC and CV of the GForm inverter was studied. The design parameters ω_n^{cc} and ω_n^{cv} were reduced a decade simultaneously from

TABLE 8 GFORM-GFEED PARTICIPATIONS

Variables	Eigenvalues														
	1	3	5	7	9	11	13	15	17	18	20	22	24	25	27
GForm Psi_{ld}	0,0003	0,0004	0,0446	0,0261	0,1467	0,0245	0	0,0243	0,0075	0,0249	0,5804	0,0003	0,3661	0,0004	0
GForm Psi_{lq}	0,0003	0,0004	0,0288	0,0632	0,0266	0,1650	0	0,0138	0,0344	0,4339	0,0109	0,0949	0,0004	0,0001	0,0001
GForm Psi_{od}	0,1142	0,1137	0,1469	0,0764	0,0295	0,0042	0	0,0004	0	0,0008	0,0187	0,0001	0,0043	0,0002	0
GForm Psi_{oq}	0,1137	0,1142	0,0886	0,1610	0,0026	0,0091	0	0,0002	0,0018	0,0179	0,0007	0,0003	0,0001	0	0,0002
GForm v_{od}	0,0050	0,0049	0,1422	0,0710	0,1887	0,0173	0	0,0065	0,0142	0,0320	0,8781	0,0014	0,9832	0,0039	0,0005
GForm v_{oq}	0,0049	0,0050	0,0918	0,1721	0,0342	0,1163	0	0,0037	0,0651	0,5403	0,0163	0,9135	0,0012	0	0
GForm P	0	0	0	0	0	0	0	0	0	0,0005	0,0002	0,0004	0,0008	0,4887	0,0328
GForm Q	0	0	0	0	0	0	0	0	0	0,0008	0,0067	0,0002	0,0138	0,5019	0,0308
GForm theta_{tot}	0	0	0	0	0	0	0	0	0	0	0	0	0	0	0
GForm x_{od}	0	0	0	0	0,0002	0,0001	0	0,0002	0,0005	0,0075	0,3947	0,0018	1,3653	0,0075	0,0008
GForm x_{oq}	0	0	0	0	0	0,0005	0	0,0001	0,0021	0,1263	0,0073	1,0659	0,0017	0,0001	0,0002
GForm x_{id}	0	0	0,0073	0,0049	0,0538	0,0135	0	0,0291	0,0157	0,0255	0,5597	0,0002	0,2273	0,0002	0
GForm x_{iq}	0	0	0,0047	0,0120	0,0098	0,0909	0	0,0165	0,0715	0,4441	0,0105	0,0671	0,0003	0	0,0001
GFeed Psi_{ld}	0	0	0,0271	0,0212	0,1753	0,1318	0,0820	0,3345	0,0027	0,0001	0,0020	0	0,0003	0	0
GFeed Psi_{lq}	0	0	0,0032	0,0044	0,0164	0,0605	0,7230	0,0376	0,0010	0,0002	0,0001	0	0	0	0
GFeed Psi_{od}	0,1143	0,1138	0,1500	0,0790	0,0042	0,0016	0	0,0454	0,0001	0,0008	0,0022	0	0,0005	0	0
GFeed Psi_{oq}	0,1137	0,1142	0,0899	0,1611	0,0079	0,0294	0	0,0029	0,0031	0,0008	0,0004	0,0002	0,0001	0	0
GFeed v_{od}	0,0050	0,0050	0,1881	0,1063	0,1553	0,0237	0	0,0448	0,0050	0,0004	0,0145	0,0001	0,0033	0,0001	0,0001
GFeed v_{oq}	0,0049	0,0050	0,0921	0,1570	0,0504	0,2139	0	0,0217	0,0245	0,0353	0,0013	0,0058	0,0003	0,0006	0,0002
GFeed v_{pll}	0	0	0,0001	0,0003	0,0006	0,0083	0	0,0054	1,0109	0,1639	0,0040	0,0511	0,0014	0,0029	0,0028
GFeed x_{pll}	0	0	0	0	0	0,0001	0	0	0,0070	0,0282	0,0014	0,0496	0,0017	0,0951	1,0540
GFeed theta_{tot}	0	0	0,0002	0,0007	0,0005	0,0063	0	0,0024	0,2543	0,4103	0,0150	0,2836	0,0077	0,0260	0,1190
GFeed x_{id}	0	0	0,0055	0,0050	0,0796	0,0895	0,0820	0,4899	0,0045	0,0001	0,0019	0	0,0002	0	0
GFeed x_{iq}	0	0	0,0007	0,0010	0,0075	0,0411	0,7230	0,0551	0,0016	0,0002	0,0001	0	0	0	0
Load Psi_r	0,0221	0,0220	0,0010	0,0005	0,1743	0,0106	0	0,2468	0,0014	0,0027	0,0377	0,0008	0,0084	0,0004	0,0001
Load Psi_i	0,0220	0,0221	0,0006	0,0010	0,0617	0,3217	0	0,0227	0,1589	0,0701	0,0128	0,0130	0,0029	0,0003	0
Netw v_{br}	0,2406	0,2396	0,0005	0,0002	0,0165	0,0023	0	0,0032	0,0003	0	0,0014	0	0,0003	0	0
Netw v_{bi}	0,2396	0,2407	0,0003	0,0005	0,0040	0,0178	0	0,0017	0,0018	0,0019	0,0001	0,0004	0	0	0

1000-250 rad/s and 100-25 rad/s, respectively. Fig. 8 shows the impact of varying the bandwidth in the eigenvalue locus diagram. In Table, some poles move towards the unstable region as the control of the GForm is slowed down, especially, modes 5 and 7 but without turning unstable. Results show that control interactions between GForm and GFeed inverter exist, but they do not destabilize the system.

B. *Grid Former – Grid Former.*

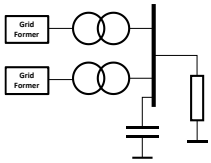

Fig. 9 Single line diagram for GForm-GForm configuration.

Fig. *9* shows the single line diagram of the GFrom inverter – GForm inverter configuration. The inverters are connected in parallel to a single bus with a series inductance and resistance in parallel with a capacitor load with the parameters in Table 9. Parameters of both GForm inverters are shown in Table 3. Initial active and reactive power injections of the GForm inverters are 0.5 and 0.324 pu respectively. The load is such that it consumes the active power provided by the inverters and the reactive power is compensated to obtain a bus voltage of 1 pu.

TABLE 9 NODE VALUES

Parameter		Value
Z	R_s	$0.7288\ pu$
	L_s	$0.4446\ pu$
C		$0.0100\ pu$

Table 10 and Table 11 show the complex and real eigenvalues of system shown. This time, a positive real value can be found, indicating that the system is unstable.

This instability can be further studied by analyzing the participation factors shown in Table 12. The unstable eigenvalue is mainly influenced by the inverter-output current and CC-related state variables $\{\boldsymbol{x}_d^o, \boldsymbol{x}_q^o, \boldsymbol{x}_d^i, \boldsymbol{x}_q^i\}$.The fact that both inverters variables intervene in that eigenvalue with similar participation factor values suggests that the instability is provoked by the control interactions. Indeed, when only analyzing a single GForm inverter connected to the RLC load, the system is stable as shown in Fig. *10* using the same set of parameters of Table 4 for GForm and a load R_s, L_s and C with values in pu of 1.4447, 0.8957 and 0.01 pu, respectively.

TABLE 10 COMPLEX EIGENVALUES

Complex				
No.	Real	Imag.	Damp. (%)	Freq. (Hz)
1	-43,88	19461,00	0,23	3097,31
3	-43,89	18832,73	0,23	2997,32
5	-682,56	4445,67	15,18	707,55
7	-678,02	3838,00	17,40	610,84
9	-811,01	1580,67	45,65	251,57
11	-692,27	1063,02	54,57	169,18
13	-149,99	140,96	72,87	22,43
15	-90,73	46,05	89,17	7,33
17	-82,80	15,71	98,25	2,50
19	42,52	46,72	-67,31	7,44
21	-47,79	14,98	95,42	2,38
23	-27,62	39,49	57,32	6,28
26	-8,86	32,46	26,32	5,17

TABLE 11 REAL EIGENVALUES

Real	
No.	Real
25	-35,34
28	-20,97
29	-19,89

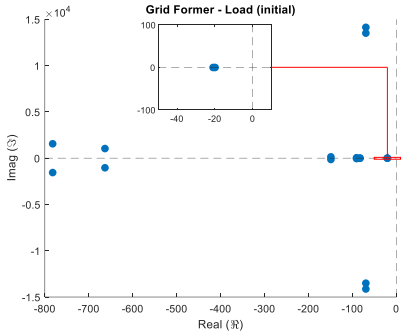

Fig. 10. Eigenvalue locus of GForm standalone operation in island.

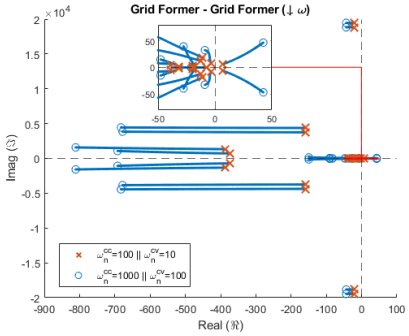

Fig. 11 Eigenvalue locus trajectories in function of the reduction of the control bandwidth for both Gform in a GForm-GForm system.

TABLE 12 GFORM-GFORM PARTICIPATIONS

Variables	Eigenvalues															
	1	3	5	7	9	11	13	15	17	19	21	23	25	26	28	29
GForm1 Psi_{ld}	0,0004	0,0004	0,0381	0,0435	0,0908	0,1142	0,1662	0,0899	0,0827	0,0782	0,1036	0,0954	0,0074	0,0135	0,0001	0
GForm1 Psi_{lq}	0,0004	0,0004	0,0381	0,0435	0,0908	0,1142	0,1673	0,0796	0,0839	0,0768	0,1039	0,0946	0,0063	0,0161	0	0
GForm1 Psi_{od}	0,1178	0,1178	0,1191	0,1174	0,0046	0,0038	0,0056	0,0009	0,0007	0,0225	0,0047	0,0108	0,0010	0,0053	0	0
GForm1 Psi_{oq}	0,1178	0,1178	0,1191	0,1174	0,0046	0,0038	0,0056	0,0009	0,0006	0,0222	0,0047	0,0109	0,0005	0,0058	0	0
GForm1 v_{od}	0,0053	0,0053	0,1210	0,1185	0,0868	0,0513	0,2557	0,4835	0,4435	0,0197	0,0331	0,0333	0,0441	0,0023	0,0022	0
GForm1 v_{oq}	0,0053	0,0053	0,1210	0,1185	0,0868	0,0513	0,2573	0,4098	0,5179	0,0240	0,0593	0,0398	0,0003	0,0032	0	0
GForm1 P	0	0	0	0	0	0	0,0001	0,0001	0,0001	0,0230	0,0337	0,0685	0,0021	0,2357	0,0174	0,4826
GForm1 Q	0	0	0	0	0	0	0,0012	0,0080	0,0091	0,0261	0,0502	0,0662	0,2347	0,0093	0,4769	0,0174
GForm1 theta_{tot}	0	0	0	0	0	0	0	0	0	0	0	0	0	0	0	0
GForm1 x_{od}	0	0	0	0	0,0002	0,0005	0,0437	0,3312	0,4398	0,0471	0,0591	0,1082	0,2001	0,0167	0,0042	0
GForm1 x_{oq}	0	0	0	0	0,0002	0,0005	0,0443	0,2841	0,5227	0,0433	0,1701	0,1235	0,0018	0,0205	0	0
GForm1 x_{id}	0	0	0,0063	0,0083	0,0416	0,0774	0,1818	0,0756	0,0595	0,1021	0,0491	0,0815	0,0009	0,0161	0	0
GForm1 x_{iq}	0	0	0,0063	0,0083	0,0416	0,0774	0,1831	0,0669	0,0603	0,1003	0,0492	0,0808	0,0007	0,0191	0	0
GForm2 Psi_{ld}	0,0004	0,0004	0,0381	0,0435	0,0908	0,1142	0,1662	0,0899	0,0827	0,0782	0,1036	0,0954	0,0074	0,0135	0,0001	0
GForm2 Psi_{lq}	0,0004	0,0004	0,0381	0,0435	0,0908	0,1142	0,1673	0,0796	0,0839	0,0768	0,1039	0,0946	0,0063	0,0161	0	0
GForm2 Psi_{od}	0,1178	0,1178	0,1191	0,1174	0,0046	0,0038	0,0056	0,0009	0,0007	0,0225	0,0047	0,0108	0,0010	0,0053	0	0
GForm2 Psi_{oq}	0,1178	0,1178	0,1191	0,1174	0,0046	0,0038	0,0056	0,0009	0,0006	0,0222	0,0047	0,0109	0,0005	0,0058	0	0
GForm2 v_{od}	0,0053	0,0053	0,1210	0,1185	0,0868	0,0513	0,2557	0,4835	0,4435	0,0197	0,0331	0,0333	0,0441	0,0023	0,0022	0
GForm2 v_{oq}	0,0053	0,0053	0,1210	0,1185	0,0868	0,0513	0,2573	0,4098	0,5179	0,0240	0,0593	0,0398	0,0003	0,0032	0	0
GForm2 P	0	0	0	0	0	0	0,0001	0,0001	0,0001	0,0230	0,0337	0,0685	0,0021	0,2357	0,0174	0,4826
GForm2 Q	0	0	0	0	0	0	0,0012	0,0080	0,0091	0,0261	0,0502	0,0662	0,2347	0,0093	0,4769	0,0174
GForm2 theta_{tot}	0	0	0	0	0	0	0	0	0	0,0568	0,0423	0,1141	0,0017	0,4807	0	0
GForm2 x_{od}	0	0	0	0	0,0002	0,0005	0,0437	0,3312	0,4398	0,0471	0,0591	0,1082	0,2001	0,0167	0,0042	0
GForm2 x_{oq}	0	0	0	0	0,0002	0,0005	0,0443	0,2841	0,5227	0,0433	0,1701	0,1235	0,0018	0,0205	0	0
GForm2 x_{id}	0	0	0,0063	0,0083	0,0416	0,0774	0,1818	0,0756	0,0595	0,1021	0,0491	0,0815	0,0009	0,0161	0	0
GForm2 x_{iq}	0	0	0,0063	0,0083	0,0416	0,0774	0,1831	0,0669	0,0603	0,1003	0,0492	0,0808	0,0007	0,0191	0	0
Load Psi_r	0,0145	0,0145	0	0	0,1550	0,1330	0,1659	0,0279	0,0195	0	0	0	0	0	0,0006	0
Load Psi_i	0,0145	0,0145	0	0	0,1550	0,1330	0,1669	0,0273	0,0175	0	0	0	0	0	0,0006	0,0001
Netw v_{br}	0,2395	0,2395	0	0	0,0118	0,0115	0,0012	0,0004	0,0002	0	0	0	0	0	0	0
Netw v_{bi}	0,2395	0,2395	0	0	0,0118	0,0115	0,0012	0,0004	0,0002	0	0	0	0	0	0	0

As the state variables affected correspond to the inner controls, the modification of the controller bandwidths could move the poles to a stable region. Again, the design parameters ω_n^{cc} and ω_n^{cv} are reduced a decade simultaneously from 1000-250 rad/s and 100-25 rad/s, respectively.

Fig. *11* shows the impact of varying the bandwidth in the eigenvalue locus diagram. It can be seen how the positive pole moves towards the stable region. Other modes move towards the unstable region. However, the system is never stable.

Finally, the control bandwidth of only one of the Grid Formers is modified. Fig. *12* shows the impact on varying the bandwidth of GForm1 on the eigenvalue locus. Fig. *12* also shows how the most critical poles (those close to the imaginary axis) move very much like in Fig. *11* while less critical poles (further away from the imaginary axis) move a shorter distance.

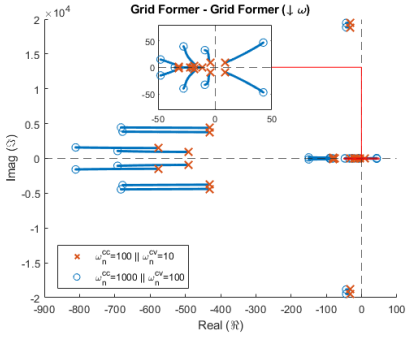

Fig. 12 Eigenvalue locus trajectories in function of the reduction of the control bandwidth of just one GForm for GForm-GForm system.

Results show that the design methodology used (often used in the literature) does not necessarily lead to a stable system when two identical GForm inverters are connected in parallel and their control parameters are adjusted in the same way, although the system is stable with only one GForm connected. The unstable mode seems to move to the stable region when slowing down the closed-loop response.

V. CONCLUSION

This paper has investigated control interactions of inverters operating in islanded mode. Specifically, the impact of the control bandwidth of the inner current and voltage control loops has been assessed. Controllers have been systematically tuned by using a pole placement methodology. The assessment is based on a modal analysis. Two cases have been addressed: The assessment has been carried out for two system configurations: (a) a grid-feeding (GFeed) inverter in parallel with a grid-forming (GForm) inverter connected to load and (b) two GForm inverters in parallel connected to a load. Results have shown that the GFeed-GForm configuration is stable, even with varying control bandwidths of the GForm inverter. The GForm-GForm configuration is not stable due to control iterations although a single GForm inverter connected to the load is stable. Thus, control interactions need to be considered when tuning control parameters.

VI. REFERENCES

[1] F. J. Pazos, «Operational Experience and Field Test on Islanding Events Cuased by a Large Photovoltaic Plants», *21st Int. Conf. Electr. Distrib.*, n.º 0184, pp. 1-4, jun. 2011.

[2] J. C. Vasquez, J. M. Guerrero, P. Rodríguez, y R. Teodorescu, «Adaptive Droop Control Applied to Voltage-Source Inverters Operating in Grid-Connected and Islanded Modes», *IEEE Trans. Ind. Electron.*, vol. 56, n.º 10, p. 10, 2009.

[3] S. D'Arco, J. A. Suul, y O. B. Fosso, «Automatic Tuning of Cascaded Controllers for Power Converters Using Eigenvalue Parametric Sensitivities», *IEEE Trans. Ind. Appl.*, vol. 51, n.º 2, pp. 1743-1753, mar. 2015, doi: 10.1109/TIA.2014.2354732.

[4] T. Qoria, F. Gruson, F. Colas, X. Guillaud, M.-S. Debry, y T. Prevost, «Tuning of Cascaded Controllers for Robust Grid-Forming Voltage Source Converter», en *2018 Power Systems Computation Conference (PSCC)*, Dublin, Ireland, jun. 2018, pp. 1-7, doi: 10.23919/PSCC.2018.8443018.

[5] C. Bajracharya y M. Molinas, «Understanding of tuning techniques of converter controllers for VSC-HVDC», *Nord. Workshop Power Ind. Electron.*, pp. 1-9, jun. 2008.

[6] T. Qoria, Q. Cossart, C. Li, X. Guillaud, F. Gruson, y X. Kestelyn, «WP3 - Control and Operation of a Grid with 100% Converter-Based Devices», p. 89.

[7] N. Pogaku, M. Prodanovic, y T. C. Green, «Modeling, Analysis and Testing of Autonomous Operation of an Inverter-Based Microgrid», *IEEE Trans. Power Electron.*, vol. 22, n.º 2, pp. 613-625, mar. 2007, doi: 10.1109/TPEL.2006.890003.

[8] U. Markovic, O. Stanojev, E. Vrettos, P. Aristidou, y G. Hug, «Understanding Stability of Low-Inertia Systems», engrXiv, preprint, feb. 2019. doi: 10.31224/osf.io/jwzrq.

[9] I. Perez-arriaga, G. Verghese, y F. Schweppe, «Selective Modal Analysis with Applications to Electric Power Systems, PART I: Heuristic Introduction», *IEEE Trans. Power Appar. Syst.*, vol. PAS-101, n.º 9, pp. 3117-3125, sep. 1982, doi: 10.1109/TPAS.1982.317524.